Metabolite Profiles of Energy Cane and Sugarcane Reveal Different Strategies During the Axillary Bud Outgrowth

Luís Furlan de Abreu
State University of Campinas
Nicholas Silva
State University of Campinas
Allan Ramos Ferrari
State University of Campinas
Lucas de Carvalho
State University of Campinas
Marcelo Falsarella Carazzolle
State University of Campinas
Taícia Pacheco Fill
State University of Campinas
Eduardo Pilau
State University of Maringa
Gonçalo Guimarães Pereira (goncalo@unicamp.br)
Laboratory of Genomics and BioEnergy (LGE), Institute of Biology, Department of Genetics, Evolution, and Bioagents, Campinas State University (UNICAMP), 13083-864 Campinas, SP, Brazil.
Maria de Barros Grassi
State University of Campinas

Research Article

Keywords: Sugarcane, pre-sprouted seedlings (PSS), phenylpropanoid pathway, electron transport

Posted Date: December 17th, 2020

DOI: https://doi.org/10.21203/rs.3.rs-126659/v1

Abstract

Sugarcane (*Saccharum* spp.) is one of the most well-known plants which possesses a large accumulation of sucrose. Another cultivar, energy cane, is an interspecific hybrid with higher fiber and lower sugar content than sugarcane. Commercial cultivation of sugarcane and energy cane is carried out by vegetative propagation, through the distribution of culm segments (setts) or pre-sprouted seedlings (PSS). In this context, the metabolism of axillary bud outgrowth is crucial for cultures that use vegetative propagation. In this work, we evaluate the metabolic profile of sugarcane and energy cane in the early hours during the axillary bud outgrowth. Sugarcane showed few metabolic changes, except for the significant increase in glutamate levels, which may be associated with root formation in the culm. In contrast, energy cane presented significant changes in amino acid catabolism, increased levels of reducing sugars, lipids, and metabolite activity in the phenylpropanoid pathway. These results together reveal changes in the energy and redox status of the cell, electron transport for the TCA cycle, and an increase in compounds related to cell wall formation and growth in energy cane. Our study provides new insights on the regulation of the axillary bud of species of the *Saccharum* complex.

1. Introduction

Sugarcane (*Saccharum* spp.) stands out among the main crops in the world, especially in countries with tropical and subtropical climates, for the production of sugar and ethanol. It is a crop of great interest, due to its energy and biomass conversion efficiency. In the last decades, breeding programs had as main objective the increase of sucrose in the culms. However, recent advances in industrial technologies and in biotechnology have made possible the fermentation of soluble sugars generated from the deconstruction of biomass (cellulose and hemicellulose), producing the so-called second-generation ethanol[1,2]. In this context, the selection of hybrids with high amounts of biomass resulted in individuals twice as productive as sugarcane. These hybrids, known as energy cane[3], are an interspecific hybrid arising from backcrossing two species, *S. spontaneum* and *S. officinarum*, generating a plant with higher fiber and lower sugar content than sugarcane[4]. The morphological characteristics of energy cane results in a crop with greater potential for biomass production when compared to sugarcane. Such performance is mainly due to the high density of the plant, high sprouting rate, faster growth and development, tillering rate, root volume, and biomass accumulation[4,5,6].

Commercial cultivation of sugarcane and energy cane is carried out through vegetative propagation. Traditionally, the planting of the crop is carried out by the distribution of culm segments (setts) with 3–4 buds in furrows or through the system of pre-sprouted seedlings (PSS) - culm cutting around the node containing one axillary bud[7]. The regulation of axillary bud outgrowth is crucial for cultures that use vegetative propagation. The buds are axillary meristems composed of cells and tissues in a state of latency and with great power of differentiation[8]. In most plant species, the axillary buds are dormant and, although meristems are fully developed, there is no division and cell growth[9]. The state of dormancy can be characterized based on three factors: i) when it is due to the internal state of the bud, known as endo-

dormancy; ii) when there is endogenous signaling to bud from other organs, such as hormonal signaling, known as para-dormancy; and iii) when there are external stimuli to the plant such as temperature variation, photo-period, availability of water and nutrients, which is known as eco-dormancy[10,11]. Therefore, the shoot branching pattern depends not only on the initiation of the axillary meristems, but also on the regulation of bud outgrowth which, in turn, is crucial to control shoot architecture and biomass production[12].

The regulation of the axillary bud is governed by a complex interaction between environmental, genetic and metabolite factors[13]. Changes in metabolite signals from other regions of the plant are detected before axillary bud outgrowth begins[14]. Moreover, several hormones play an important role as the main regulatory molecules during axillary bud outgrowth, among which auxin, cytokinin and strigolactone stand out[11,12,15]. Furthermore, the cellular energy for growth can be provided through glycolysis and amino acids fed in the TCA cycle[16,17]. Sugars and amino acids are part of a sophisticated metabolic network, linking energy status and regulating growth[16]. Studies in plant metabolism have focused on elucidating the function and regulation of certain biosynthetic pathways[18]. In this context, metabolomics has been used as a tool to elucidate the mechanisms involved in metabolic regulation, as well as to understand the interaction between genotype and phenotype[19]. Recently, metabolites in bud and culm portions of 16 sugarcane cultivars have been associated with cultivars with a high sprouting rate[20]. In addition, the metabolic profile of energy cane setts treated with auxin (bud sprouting inhibitor), revealed metabolites associated with presence of oxygen and energy status during bud outgrowth[21]. However, key markers that regulate axillary bud outgrowth remain largely unknown.

In the present study, we evaluated changes in the metabolic profile during the axillary bud outgrowth of sugarcane and energy cane and verified different strategies used for each cultivar during the first hours of the axillary bud outgrowth. Our result results demonstrate greater metabolic activity during the axillary bud outgrowth in energy cane compared to sugarcane. Also, the key metabolites contributions to the dormancy process and the mechanism of the sprouting process of species of the *Saccharum* complex are introduced, providing insights for future molecular and agricultural research.

2. Results

2.1. Sprouting rate and shoot height

Commercial cultivars of sugarcane (9 month-old CTC 4) and energy cane (9 month-old Vertix 12) were used in this study. The + 3 to + 14 internodes were randomly selected. The setts were planted individually in trays and were evaluated for the progress of emergence (Emergence Velocity Index – EVI) for each bud. It was considered it to have sprouted when the shoot emerged from the vermiculite, and shoot height was evaluated. After 30 days, the energy cane presented twice the EVI of sugarcane (Fig. 1A) and shoot height of 34.12 ± 4.33 cm compared to 7.43 ± 2.79 cm of sugarcane (Fig. 1B). With only eight days of planting, 83.33% of the energy cane setts had sprouted, with the average shoot height of 8.08 ± 1.69 cm, however,

in sugarcane only 25.0% of the buds had sprouted, with average shoot height of 0.36 ± 0.69 cm (data not shown).

2.2. Analysis of GC-TOF-MS reveals difference in the metabolism of axillary bud outgrowth of energy cane and sugarcane

To unravel the differential metabolome of the axillary bud outgrowth of energy cane and sugarcane, five buds from both cultivars were randomly collected at 0 and 48 hours after planting resulting in a total of 20 samples. GC-TOF-MS analysis allowed us to identify a total of 46 metabolites, which included amino acids, sugars, and organic acids (Table S1 and Fig. S2. Supplementary information). The identified metabolites are involved in several metabolic pathways, such as the tricarboxylic acid (TCA) cycle, glycolysis, amino acid biosynthesis, organic acid biosynthesis and phenylpropanoid biosynthesis. Multivariate statistical analysis of metabolite data through Principal Component Analysis (PCA) showed clear discrimination among axillary bud outgrowth in energy cane (Fig. 2A), however, in sugarcane this difference was not so clear (Fig. 2B). Similarly, partial least squares-discriminant analysis (PLS-DA) of metabolites during the axillary bud outgrowth showed separate grouping for each time in energy cane (Fig. 2C) and sugarcane (Fig. 2D).

Next, we sought to verify the metabolic changes during the axillary bud outgrowth. In energy cane, 20 metabolites were found to be differentially changed between 0 and 48 hours ($p \leq 0.05$). Methionine, lysine, arginine, tryptophan, ornithine, glycine, alanine, isoleucine, raffinose, GABA (γ – aminobutyric), and lactate showed reduced levels from 0 to 48 hours. In contrast, nine metabolites increased their levels according to bud outgrowth: pyroglutamate, chorismate, aspartate, quinate, ferulate, fucose, fructose, aconitate and *myo*-inositol. In contrast, in sugarcane it was possible to observe differential changes only in the levels of glutamate, induced after 48 hours (Fig. 3). Our results provide the first molecular clues to the sprouting rate and shoot height differences observed between a cultivar of energy cane and sugarcane.

To further investigate the metabolic pathways that modulate the bud outgrowth in energy cane and sugarcane, a pair-wise comparison between growth times 0 and 48 hours for each cultivar were performed. We observed significant metabolite changes ($p \leq 0.05$), as depicted on the metabolic map (Fig. 4). In energy cane, there was a significant increase in fructose (0.876 fold), *myo* – inositol (0.952 fold), quinate (0.836 fold), chorismate (0.887 fold), ferulate (0.833 fold), aspartate (0.949 fold), aconitate (0.933 fold), fucose (0.867 fold), and pyroglutamate (0.894 fold). However, we verified a significant reduction in the levels of raffinose (1.156 fold), glycine (1.082 fold), lactate (1.218 fold), alanine (1.135 fold), lysine (1.19 fold), methionine (1.049 fold), isoleucine (1.082 fold), tryptophan (1.147 fold), GABA (1.205 fold), ornithine (1.128 fold), and arginine (1.343 fold). During the bud outgrowth in sugarcane, we observed statistically significant changes only in the levels of glutamate (0.823 fold increase). Together, these results suggest key different strategies during the axillary bud outgrowth of the two cultivars. Moreover, even after 48 hours of sugarcane planting, the axillary bud outgrowth and metabolic changes were not verified, which indicates that the axillary bud is in the dormant phase.

In addition, to define metabolic changes related to the sprouting process in the energy cane, the pairwise Pearson correlation coefficient was analyzed for each metabolite. Metabolites involved in the phenylpropanoids biosynthesis showed strong positive correlation when paired against each other. On the other hand, we verified a strong negative correlation between some amino acids, among them pyroglutamate (Fig. S3). Clearly, these findings suggest that during the axillary bud outgrowth, there was an increase in sugar metabolism and phenylpropanoids biosynthesis and a decrease in amino acid metabolism.

2.3. Major response related to LC-ESI(+)-MS/MS analysis

Untargeted LC-ESI(+)-MS/MS analysis was performed as a complementary approach to describe the changes in metabolism during the axillary bud outgrowth. PCA and PLS-DA of metabolites showed separate grouping in energy cane, however in sugarcane we did not observe the same result (Fig. 5). In total, 35 compounds were detected in the bud's samples (Fig. 6A) (Table S2 and Fig. S2. Supplementary information). Among these metabolites, eight were common between the two approaches and had the same concentration profile: phenylalanine, caffeate, tyrosine, asparagine, glutamate, pyroglutamate, leucine, and chorismate (Fig. 6B).

Next, we performed two-way ANOVA analysis of the metabolic profile between the two cultivars in relation to time (*p*-value = 0.00792) and in relation to cultivars only (*p*-value = 0.00328). The cultivar and time interaction proved to be significantly different (*p*-value = 0.00181), which indicates the relationship of the cultivar and the relative quantification of metabolites is time-dependent. Moreover, we can notice two groups of metabolites clearly different in both cultivars where 16 metabolites demonstrated to have higher concentrations in energy cane, which includes organic acids, lipids, choline derivatives, amino acids or derivatives. While a group of 12 metabolites were less concentrated in energy cane than in sugarcane, which mostly includes sugars (Fig. 6A).

3. Discussion

Sprouting is an important stage of development which is regulated for axillary bud outgrowth being a central process for establishing the crops that are planted through vegetative propagation[22]. We verified the sprouting capacity of a cultivar of energy cane and sugarcane. The emergence velocity index, followed by a faster shoot development, was clearly higher in energy cane (Fig. 1). Energy cane demonstrates greater capacity and homogeneity of sprouting of all internodes[6], and a higher sprouting rate when treated with auxin previous to planting[21]. The faster shoot development of energy cane (Fig. 1B) can be associated with two factors: (i) early shoot development followed by the roots formation, which suggests an early onset of the photosynthetic process while the opposite is observed in sugarcane; and (ii) the higher rate of nocturnal growth of energy cane compared to sugarcane[6]. These data can suggest a differentiated metabolism in the axillary bud of energy cane, which contributes to a rapid axillary bud outgrowth.

Metabolomics has been used as a great molecular tool, able to help unravel mechanisms of plant metabolism during growth. Integration of both GC-TOF-MS and LC-ESI-MS/MS allows to identify a set of metabolites involved in several aspects of plant development, plant pathogen interaction, and abiotic stress conditions[23]. Here, we present the metabolites' relative abundance during the axillary bud outgrowth (0 and 48 hours) of energy cane and sugarcane, and associate these data with metabolic pathways. We found a prevalence of reducing sugars (glucose and fructose) in energy cane while in sugarcane a trend in the reduction of the levels of these sugars was verified. During the axillary bud outgrowth, there is a decrease in the concentration of sucrose and an increase of hexoses[24]. Interestingly, a greater performance of a sprouting process is associated with low levels of sucrose present in the culms[25]. In energy cane, the low levels of sucrose and consequent high levels of reducing sugars suggest that glucose and fructose play an important role in regulating bud outgrowth when they are rapidly synthesized and metabolized. Furthermore, axillary buds are centers of meristematic activity, which exhibits a high rate of metabolism, thus requiring a range of soluble carbohydrates for the sprouting process. These metabolites can be translocated to buds through source organs, such as culms, causing a progressive tissue increase[26]. Culm metabolism is extremely important in determining axillary bud outgrowth or dormancy status[27]. The metabolic profile of sugarcane culm and bud revealed that the metabolic network of culm is more coordinated than that of bud. Besides that, glutamate and serine are metabolites that present a clear connection between the two tissues[20].

The role of amino acids in plant metabolism is fundamental for a multitude of metabolic reactions related to various physiological processes, such as plant growth and development, generation of metabolic energy or redox power, and resistance to abiotic and biotic stress[28,29,30]. We found differences in abundant levels of amino acids during the axillary bud outgrowth and overall were highly correlated. We identified changes in levels of amino acids associated with ASP-famliy pathway (AFP) such as lysine, isoleucine, and methionine of which aspartate is a precursor[16,17,31]. Lysine and isoleucine catabolism in the TCA cycle allows continuous operation of the mitochondrial electron transport chain under limited energy or carbon availability[31]. Moreover, methionine is a fundamental metabolite in plants, once the majority of this amino acid is converted to S-adenosylmethionine (SAM) which regulates a range of biological processes, such as the formation of cell wall, syntheses of ethylene, vitamin, and polyamines[17,31]. Ethylene has demonstrated a great activator for the development of axillary bud in sugarcane[8]. In energy cane, we verified an increase in aspartate and a reduction in the levels of the lysine, isoleucine and methionine, which suggest the catabolism of these amino acids to supply electrons for the TCA cycle and for the formation of SAM during axillary bud outgrowth. In sugarcane, we see an increase in the levels of lysine, threonine, and methionine, that is a consequence of the high levels of glutamate. In *Arabidopsis thaliana*, high concentrations of lysine cause a delay in breaking seed dormancy[32], which corroborates to our results in sugarcane.

Another amino acid with an important role in regulating plant metabolism is glutamate, being a primary product of nitrogen assimilation[33]. Glutamate plays a very important role in the plant signaling and in the

construct of root architecture in arabidopsis[34,35] and is a metabolite that acts as a crosstalker between bud and culm of sugarcane[20]. Our data show a significant increase in glutamate during the axillary bud outgrowth in sugarcane. Taken together, we hypothesized that increased levels of glutamate in the bud may act as a signaling molecule in the culm for root formation on the setts (morphologically similar to secondary roots). After planting the sugarcane, the root formation occurs after 24 hours[36]. However, energy cane has shown to have a different development strategy, with shoot development first and then root formation 10 days after planting[6].

In addition, it is well known that glutamate is a precursor to the synthesis of proteins, polypeptides, and organic compounds. These organic compounds include proteinogenic amino acids, such as glutamine, proline, arginine, histidine and non-proteinogenic amino acids, such as GABA[37,38,39]. The synthesis of GABA can occur through two alternative routes: (i) glutamate can be transported to the cytoplasm, where is degraded into GABA, which is subsequently imported into the mitochondria to be converted as a final product into succinate in the TCA cycle, regulating the redox balance and metabolism energy[28,40]; (ii) ornithine and arginine catabolism results in the formation of putrescine, through enzymes decarboxylases. Putrescine is then converted into spermidine and spermine, and then into GABA in the cytoplasm[41]. GABA can act as signaling molecule in plant growth and development[42,43,44] and plays an important role during seed germination, providing, through the TCA cycle, building blocks for metabolic reorganization, prior to the degradation of energy-demanding storage reserves[39]. In energy cane, we observe an increase in the catabolism of GABA, ornithine, arginine, and ASP-family amino acids, which taken together results in an increased activity in the TCA cycle, providing increased electron transport and energy during the axillary bud outgrowth. The reduction in GABA levels has also been reported in bud outgrowth of setts of energy cane under water soaking[21].

Moreover, in energy cane we observe a reduction in pyruvate, alanine and lactate levels. In sugarcane, we observed a reduction only in lactate levels. Lactate synthesis is controlled by the pH of the cytosol under hypoxia where it is initially converted to lactate but, as the pH decreases, an accumulation of ethanol occurs in the cell[45]. The formation of alanine diverts carbon to neutral amino acids, preventing cell acidification and carbon loss[28]. Energy cane setts under the auxin stimulus showed an increase in lactate levels resulting in a delay in the bud sprouting process, possibly caused by cell acidification[21]. The low levels of lactate may be an indication that this metabolite is a possible repressor for the axillary bud outgrowth, since cellular acidity can cause hypoxia[46]. Furthermore, oxygenation may be a first clue to the transition from breaking dormancy and developing the axillary meristem[47]. Molecular oxygen is essential for the formation of ATP, serving as a terminal electron acceptor for the transport chain in the TCA cycle and providing energy for growth.

Metabolites associated with cell growth and expansion are related to the phenylpropanoid pathway. In energy cane, we verified an increase in the levels of p-coumarate, caffeate, and ferulate during the bud outgrowth. Phenylpropanoids are necessary for the biosynthesis of a large number of metabolites, including flavonoids, hydroxycinnamate esters (HCEs), wall-linked hydroxycinnamic acids (HCAs) and

lignins[48,49]. In most plants, the first step in the pathway of phenylpropanoids is the deamination of phenylalanine in cinnamate by L-phenylalanine ammonia lyase (PAL; EC 4.3.1.24). However, it has been shown that the grasses of the Poaceae family (or Gramineae, also known as true grasses) and to a lesser extent to some orders of dicotyledonous plants, such as Fabales, Malvales, Asterales, Caryophyllales, ferns, and Solanales use a more efficient route than dicots. In this pathway, tyrosine is directly transformed into p-coumarate by phenylalanine / tyrosine (bifunctional) ammonia lyase (PTAL; EC 4.3.1.25)[49,50,51]. Caffeate and ferulate are precursors to most lignins, lignans, and are associated with suberin and cutin polymer matrix waxes[51,52,53]. Ferulate is found as a component of the cell wall and is considered important to increase the rigidity and strength of the cell wall and conduction vessels in grasses[54,55], dicots[56] and gymnosperms[57]. In these cell walls, ferulate serves as an initiation site for lignification, acting as a crosslinking system for arabinoxylans and lignins[49,54,58,59,60]. It is proposed in grasses that the formation of cross-linked between ferulate, arabinoxylans and lignin, is the mechanism by which cells end the elongation process, alternating from the development of the primary to the secondary wall[58,61]. Monocotyledons have a unique cell wall composition, showing high proportions of type S lignin, hydroxycinnamates (ferulate and p-coumarate) attached to the cell wall and the presence of tricin flavonoid[62]. Furthermore, ferulate is the main hydroxycinnamic derivative of young cell walls while p-coumarate is an indicator of cell wall maturity, since it is esterified mainly in side chains of S units and its incorporation follows the same deposition pattern syringe units[63,64,65]. In addition to their role in the plant wall, phenolic compounds are often associated with improved redox status and antioxidant protection of cells, acting in the elimination of reactive oxygen species (ROS)[49,66].

Breaking dormancy in the axillary meristem is a process that requires energy to trigger cell division and elongation[12]. For such processes, ascorbate biosynthesis plays a fundamental role[67]. However, *myo*-inositol and galacturonate are metabolites that interconnect ascorbate biosynthesis, promoting cell division and elongation[67]. *Myo*-inositol is an important cellular metabolite that forms the structural basis of a series of lipid signaling molecules that function in several pathways, including responses to stress, regulation of cell death, biosynthesis of secondary metabolites and phytohormones[68]. Among the phytohormones, cytokinins play an important role in the regulation of axillary bud outgrowth, which in turn are controlled by auxins through the process of apical dominance (para-dormancy)[10,11]. Our data demonstrate that during the axillary bud outgrowth in the energy cane, there is a significant increase in the levels of *myo*-inositol and metabolites of the phenylpropanoid pathway, which together may be correlated to the process of division, elongation and cell growth.

Growth and development processes are closely linked to lipid biosynthesis. During cell growth, there is an increase in lipid metabolism[69]. Lipids are vital cellular constituents because they provide the structural basis for membranes and energy storage for metabolism[70]. Phospholipid bilayers maintain the structure and functionality of all membrane systems[70]. In this context, choline is a key metabolite precursor to phospholipid and plays an important role as osmoprotectant, improving the plant growth under stress conditions[71,72]. Choline biosynthesis is derived from lipid metabolism (Kennedy pathway) where

phosphocholine is dephosphorylated to form choline[72]. Exogenous application of choline results in increased tolerance to abiotic stress in several plants[70,73,74]. In addition, it is well understood that energy cane has greater resistance to drought than other conventional cultivars[4,5]. Our LC-ESI(+)-MS data demonstrated that the metabolic profile of energy cane showed a higher relative concentration of lipid metabolism compounds and choline derivatives, which may be related to the rapid growth and greater resistance of these cultivars to abiotic stress.

In conclusion, the metabolic profile of a diverse set of compounds, such as sugars, amino acids, lipids, and organic compounds was quite evident, especially in energy cane which demonstrated a faster metabolism from sugarcane. The changes in metabolic pathways during the axillary bud outgrowth in energy cane and sugarcane is consistent to the sprouting speed observed. Remarkably, energy cane demonstrated changes in sugar levels, catabolism of amino acids, increased relative concentration of organic compounds, and greater abundance of lipids and choline derivatives which demonstrate energy production and formation of membrane and wall cells for growth. On the other hand, sugarcane showed an increase in the levels of glutamate and other amino acids, which may be related to bud dormancy and root formation in the culm. Together, our data demonstrate, for the first time, differences in the axillary bud outgrowth strategy of a cultivar of energy cane and sugarcane (Fig. 7), which may be the basis for new studies and targets for breeding programs.

4. Methods

4.1. Plant Material

Field-grown plants were harvested from Sugarcane Technology Center (CTC) and on Luiz de Queiroz Higher School of Agriculture (ESALQ), and used for preparing cane setts (one-node and single-budded). Commercial cultivars of sugarcane (9 month-old CTC 4) and energy cane (9 month-old Vertix 12) were used in this study. Setts were harvested between 9:00 and 11:00 from + 3 to + 14 internodes. The internode + 1 is connected to the first leaf with a visible dewlap, the internode count proceeds downward. The internodes were randomized to ensure similarity in natural conditions.

4.2. Growth conditions and Measurements

Sprouting and growth of setts occurred in a greenhouse (plastic-covered equipped with an exhaust fan) under natural conditions of light and temperature (22º49’09.7”S, 47º04’16.4”W). Experiments occurred in November and December, 2018. Internodes were planted in trays (38 cm length, 29 cm width, and 6.5 cm height) with vermiculite (approximately 987.9 ± 0.3 g). Bud sprouting counts were made daily through 30 days after planting (DAP) to determine the Emergence Velocity Index (EVI) using the formula described by Maguire[75]. Shoot height was measured from the ground level to the tip of the longest leaf (fully or not fully expanded) with a ruler (cm). Irrigation occurred daily so that there was no water stress. Another experiment was carried out to analyze the metabolic profile, buds from both cultivars were collected at 0 and 48 hours after planting with the aid of a scalpel (Fig. S1, Supplementary information) and

immediately frozen with liquid nitrogen for analysis of the GC-TOF-MS and LC-ESI(+)-MS/MS. A total of five biological replicas were collected, with each replicate corresponding to a pool of five different buds. The material was macerated and stored at − 80 ºC.

4.3. GC-TOF-MS analysis and Data processing

Analyses of the GC-MS of the buds were performed at the Metabolomics Laboratory (LabMet) of the National Biorenovable Laboratory (LNBR). Metabolites were extracted from 50 mg of fresh samples. Extraction solution was composed of methanol, chloroform and water (3:1:1)[76]. The 150 µl of the polar phase was dried and derivatized[77]. 1 µl of the derivatized samples were analyzed on a Combi-PAL autosampler (Agilent Technologies GmbH, Waldbronn, Germany) coupled to an Agilent 7890A gas chromatograph coupled to a Leco Pegasus HT time-of-flight mass spectrometer (LECO, St. Joseph, MI, USA)[78]. The samples were derivatized for 90 min at 30 °C with 10 µl of 40 mg ml^{-1} methoxyamine hydrochloride in pyridine followed by a 30 min treatment at 37 °C with 90 µl of N-Methyl-N-(trimethylsilyl) trifluoroacetamide (MSTFA). The gas chromatographic analysis was performed on a 30 m x 0.32 mm x 0.25 µm DB-35MS (Agilent J&W, Santa Clara, USA), the injection temperature was set at 230 °C and the ion source adjusted to 250 °C. Helium was used as the carrier gas at a flow rate of 2 ml min^{-1} under the following temperature program: 2 min of isothermal heating at 85 °C, followed by a 15 °C min^{-1} oven temperature ramp to 360 °C. Chromatograms were exported from Leco ChromaTOF software (version 4.51.6.0) to R software. Peak detection, retention time alignment, and library matching were performed using Target Search R-package[79]. Metabolites were quantified by the peak intensity of a selective mass. Metabolites intensities were normalized by dividing the fresh-weight, followed by the sum of total ion count and global outlier replacement.

4.4. LC-ESI(+)-MS/MS analysis and Data processing

Analysis of the LC-ESI(+)-MS/MS of the buds, 30 mg of fresh samples were used and extracted with a solution composed of 99.875% methanol and 0.125% formic acid[80]. The analyses were performed using ultra performance liquid chromatography (Shimadzu, Nexera X2, Japan) coupled to Mass Spectrometry (Impact II, Bruker Daltonics Corporation, Germany) and an Acquity UPLC®CSH^{TM}C18 column with 2,1 × 100 mm (Waters, Ireland), 2.1 µm of particle size and flow rate 0,200 mL min^{-1}. Mobile phase was composed of formic acid 1% in water (*v/v*) (phase A) and methanol with formic acid 0,1% (*v/v*) (phase B) at 40 ^{o}C. The analyses were performed using a Quadrupole Time-Of-Flight mass analyzer (QTOF), collision energy ramp 10–45 eV. The mass range (*m/z*) scanned was between 50 to 1400 with an acquisition rate of 7 Hz for MS and 7–12 Hz for MS/MS (ramp) in positive mode $[M + H]^{+}$with end plate offset potential − 500 V. The four most intense ions were selected for automatic fragmentation (AutoMS/MS). Spectra were processed in DataAnalysis 4.2 software.

Next, we processed spectra files with MZMine v2.53 to obtain filtered fragmentation MS2 and MS1 label-free quantification profiles files[81]. The following parameters were applied: 1) Mass detection: 1.1) MS1 level, noise level = 1E3 and 1.2) MS2 level, noise level = 5E2; 2) ADAP Chromatogram builder: 2.1) Min

Group size = 5; 2.2) Group intensity threshold = 1E3; 2.2) min highest intensity 1E4; and 2.3) m/z tolerance = 20 ppm; 3) Chromatogram deconvolution: 3.1) Algorithm wavelets (ADAP); 3.2) S/N = 10; 3.3) min feature height = 1E4; 3.4) coefficient/area = 50; 3.5) peak duration max = 2 min; 3.6) RT wavelet range = 1; 4) Isotopic peak grouper; 4.1) m/z tolerance = 20 ppm; 4.2) retention time tolerance = 0.2 min; 4.3) maximum charge = 3; 4.4) representative isotope = lowest m/z; 5) RANSAC aligner; 5.1) m/z tolerance = 20 ppm; 5.1) RT tolerance = 0.3 min; 5.2) RT after correction = 0.1 min; 5.3) RANSAC interactions = 2000; 5.4) minimum number of points = 70%; 5.5) threshold value = 0.5; 6) Gap filling peak finder; 6.1) Intensity tolerance = 30%; m/z tolerance = 20 ppm; 7) Feature list row filter; 7.1) Keep only peaks with MS2 scan; 8) Export submit to GNPS-FBMN; 8.1) Merge MS/MS; 8.2) Expected mass deviation = 20 ppm. The metabolites were identified by submission of the resulting files to GNPS[82] using both Library Search and Feature Networking modules with default parameters. Final metabolites' identification list was obtained by filtering with 1) cosine min = 0.6 and 2) MZErrorPPM max = 10 ppm.

4.5. Statistical analysis

The analysis of metabolomics data was performed using the MetaboAnalyst 4.0 software[83]. Normalization of the obtained data was carried out to remove systematic as well as replicates variation within the samples. GC-TOF-MS data were normalized using metabolite concentrations; LC-ESI(+)-MS/MS using the chromatogram area of each metabolite. Principal component analysis (PCA) and discriminant analysis (PLS-DA) were performed; mean values were transformed into log and z-score for normalization; the heat map was generated. Statistical analysis occurred within each cultivar, significantly different using Student's t-test (p-value ≤ 0.05). A two-way between groups ANOVA was used to evaluate time and variety interaction effects for dependent variables through the *aov()* function of the R 3.6.2..

Declarations

Acknowledgments

We thank Caique Camargo Malospirito for technical assistance. Sugarcane Technology Center and Luiz de Queiroz Higher School of Agriculture by the cultivars used in this study. Research supported by LNBR - Brazilian Biorenewables National Laboratory (CNPEM / MCTIC) during the use of the Metabolomics open access facility. This study was financed by the National Council for Scientific and Technological Development - Brasil (CNPq) - Finance code 140869/2016-6 to N.V.S.; São Paulo Research Foundation (FAPESP), 2018/10315-2 to L.G.F.A.; São Paulo Research Foundation (FAPESP), 2019/17007-4 to A.J.R.F.; São Paulo Research Foundation (FAPESP), 2019/12914-3 to L.M.C.

Author Contributions

L.G.F.A and N.V.S conceived, designed, performed, collected the experiments and wrote the manuscript. A.J.R.F. and L.M.C. performed MS data processing and statistical analysis. L.G.F.A., N.V.S., M.C.B.G., M.F.C. and G.A.G.P participated in compiling and interpretation of data. T.P.F. and E.J.P.

performed the LC-ESI(+)-MS/MS analyzes. All authors read and approved the final version of the manuscript.

References

1. Matsuoka, S. Journal of Scientific Achievements Free Fiber Level Drives Resilience and Hybrid Vigor in Energy Cane. *J. Sci. Achiev.* **2**, 1–35 (2017).
2. Dos Santos, L. V. *et al.* Second-Generation Ethanol: The Need is Becoming a Reality. *Ind. Biotechnol.* **12**, 40–57 (2016).
3. Viator, R. P. & Richard, E. P. Sugar and energy cane date of planting effects on cane, sucrose, and fiber yields. *Biomass and Bioenergy* **40**, 82–85 (2012).
4. Matsuoka, S., Kennedy, A. J., Santos, E. G. D. dos, Tomazela, A. L. & Rubio, L. C. S. Energy Cane: Its Concept, Development, Characteristics, and Prospects. *Adv. Bot.* 2014, 1–13 (2014).
5. Carvalho-Netto, O. V. *et al.* The potential of the energy cane as the main biomass crop for the cellulosic industry. *Chem. Biol. Technol. Agric.* **1**, 1–8 (2014).
6. de Abreu, L. G. F. *et al.* Energy cane vs sugarcane: Watching the race in plant development. *Ind. Crops Prod.* **156**, 112868 (2020).
7. May, A. *et al.* Pre-sprouted seedlings production methods through buds or mini-stems: Emergence and initial development of sugarcane cultivars. *Cientifica* **46**, 403–411 (2018).
8. Jain, R., Solomon, S., Shrivastava, A. K. & Lal, P. Nutrient application improves stubble bud sprouting under low temperature conditions in sugarcane. *Sugar Tech* **11**, 83–85 (2009).
9. Schmitz, G. & Theres, K. Shoot and inflorescence branching. *Curr. Opin. Plant Biol.* **8**, 506–511 (2005).
10. Kebrom, T. H., Brutnell, T. P., Hays, D. B. & Finlayson, S. A. Signals in the Grasses. 317–319 (2010) doi:10.1111/j.1365-3040.2009.02050.x.egetative.
11. Domagalska, M. A. & Leyser, O. Signal integration in the control of shoot branching. **12**, (2011).
12. Kebrom, T. H. A growing stem inhibits bud outgrowth – The overlooked theory of apical dominance. *Front. Plant Sci.* **8**, 1–7 (2017).
13. Huang, X., Effgen, S., Meyer, R. C., Theres, K. & Koornneef, M. Epistatic natural allelic variation reveals a function of AGAMOUS-LIKE6 in axillary bud formation in Arabidopsis. *Plant Cell* **24**, 2364–2379 (2012).
14. Barbier, F. F., Lunn, J. E. & Beveridge, C. A. Ready, steady, go! A sugar hit starts the race to shoot branching. *Curr. Opin. Plant Biol.* **25**, 39–45 (2015).
15. Dun, E. A., Germain, A. de Saint, Rameau, C. & Beveridge, C. A. Antagonistic action of strigolactone and cytokinin in bud outgrowth control. *Plant Physiol.* **158**, 487–498 (2012).
16. Galili, G. The aspartate-family pathway of plants: Linking production of essential amino acids with energy and stress regulation. *Plant Signal. Behav.* **6**, 192–195 (2011).

17. Wang, W., Xu, M., Wang, G. & Galili, G. New insights into the metabolism of aspartate-family amino acids in plant seeds. *Plant Reprod.* **31**, 203–211 (2018).
18. Fernie, A. R. & Tohge, T. The Genetics of Plant Metabolism. *Annu. Rev. Genet.* **51**, 287–310 (2017).
19. Saito, K. & Matsuda, F. Metabolomics for functional genomics, systems biology, and biotechnology. *Annu. Rev. Plant Biol.* **61**, 463–489 (2010).
20. Ferreira, D. A. *et al.* Metabolite profiles of sugarcane culm reveal the relationship among metabolism and axillary bud outgrowth in genetically related sugarcane commercial cultivars. *Front. Plant Sci.* **9**, 1–14 (2018).
21. Cunha, C. P. *et al.* Metabolic Regulation and Development of Energy Cane Setts upon Auxin Stimulus. *Plant Cell Physiol.* **0**, 1–10 (2019).
22. Baracat Neto, J., Scarpare, F. V., Araújo, R. B. de & Scarpare-Filho, J. A. Initial development and yield in sugarcane from different propagules1. *Pesqui. Agropecuária Trop.* **47**, 273–278 (2017).
23. Schaker, P. D. C. *et al.* Metabolome dynamics of smutted sugarcane reveals mechanisms involved in disease progression and whip emission. *Front. Plant Sci.* **8**, 1–17 (2017).
24. Verma, A. K., Agarwal, A. K., Dubey, R. S., Solomon, S. & Singh, S. B. Sugar partitioning in sprouting lateral bud and shoot development of sugarcane. *Plant Physiol. Biochem.* **62**, 111–115 (2013).
25. Zhu, Y. J., Komor, E. & Moore, P. H. Sucrose accumulation in the sugarcane stem is regulated by the difference between the activities of soluble acid invertase and sucrose phosphate synthase. *Plant Physiol.* **115**, 609–616 (1997).
26. Bagri, J. *et al.* Metabolic shift in sugars and amino acids regulates sprouting in Saffron corm. *Sci. Rep.* **7**, 1–10 (2017).
27. Boussiengui-Boussiengui, G., Groenewald, J. H. & Botha, F. C. Metabolic Changes Associated with the Sink-Source Transition During Sprouting of the Axillary Buds on the Sugarcane Culm. *Trop. Plant Biol.* **9**, 1–11 (2016).
28. Hildebrandt, T. M., Nunes Nesi, A., Araújo, W. L. & Braun, H. P. Amino Acid Catabolism in Plants. *Mol. Plant* **8**, 1563–1579 (2015).
29. Fagard, M. *et al.* Nitrogen metabolism meets phytopathology. *J. Exp. Bot.* **65**, 5643–5656 (2014).
30. Pratelli, R. & Pilot, G. Regulation of amino acid metabolic enzymes and transporters in plants. *J. Exp. Bot.* **65**, 5535–5556 (2014).
31. Greco, M., Chiappetta, A., Bruno, L. & Bitonti, M. B. In Posidonia oceanica cadmium induces changes in DNA methylation and chromatin patterning. *J. Exp. Bot.* **63**, 695–709 (2012).
32. Frizzi, A. *et al.* Modifying lysine biosynthesis and catabolism in corn with a single bifunctional expression/silencing transgene cassette. *Plant Biotechnol. J.* **6**, 13–21 (2008).
33. Coruzzi, G. M. Primary N-assimilation into Amino Acids in Arabidopsis. *Arab. B.* **2**, e0010 (2003).
34. Walch-Liu, P., Liu, L. H., Remans, T., Tester, M. & Forde, B. G. Evidence that L-glutamate can act as an exogenous signal to modulate root growth and branching in Arabidopsis thaliana. *Plant Cell Physiol.* **47**, 1045–1057 (2006).

35. Forde, B. G. Glutamate signalling in roots. *J. Exp. Bot.* **65**, 779–787 (2014).
36. Aude, M. I. da S. AUDE, 1993.pdf. *Ciência Rural* vol. 23 241–248 (1993).
37. Brosnan, J. T. & Brosnan, M. E. Glutamate: A truly functional amino acid. *Amino Acids* **45**, 413–418 (2013).
38. Reiner, A. & Levitz, J. Glutamatergic Signaling in the Central Nervous System: Ionotropic and Metabotropic Receptors in Concert. *Neuron* **98**, 1080–1098 (2018).
39. Qiu, X. M., Sun, Y. Y., Ye, X. Y. & Li, Z. G. Signaling Role of Glutamate in Plants. *Front. Plant Sci.* **10**, 1–11 (2020).
40. Liu, Y. & Von Wirén, N. Ammonium as a signal for physiological and morphological responses in plants. *J. Exp. Bot.* **68**, 2581–2592 (2017).
41. Shelp, B. J. *et al.* Hypothesis/review: Contribution of putrescine to 4-aminobutyrate (GABA) production in response to abiotic stress. *Plant Sci.* **193–194**, 130–135 (2012).
42. Bouché, N., Fait, A., Zik, M. & Fromm, H. The root-specific glutamate decarboxylase (GAD1) is essential for sustaining GABA levels in Arabidopsis. *Plant Mol. Biol.* **55**, 315–325 (2004).
43. Fait, A., Fromm, H., Walter, D., Galili, G. & Fernie, A. R. Highway or byway: the metabolic role of the GABA shunt in plants. *Trends Plant Sci.* **13**, 14–19 (2008).
44. Carillo, P. GABA shunt in durum wheat. *Front. Plant Sci.* **9**, 1–9 (2018).
45. Kennedy, R. A., Rumpho, M. E. & Fox, T. C. Anaerobic metabolism in plants. *Plant Physiol.* **100**, 1–6 (1992).
46. Tadege, M., Dupuis, I. & Kuhlemeier, C. Ethanolic fermentation: New functions for an old pathway. *Trends Plant Sci.* **4**, 320–325 (1999).
47. Considine, M. J. *et al.* Learning To Breathe: Developmental Phase Transitions in Oxygen Status. *Trends Plant Sci.* **22**, 140–153 (2017).
48. Anderson, N. A., Bonawitz, N. D., Nyffeler, K. & Chapple, C. Loss of FERULATE 5-HYDROXYLASE leads to mediator-dependent inhibition of soluble phenylpropanoid biosynthesis in arabidopsis. *Plant Physiol.* **169**, 1557–1567 (2015).
49. Aguiar, N. O., Olivares, F. L., Novotny, E. H. & Canellas, L. P. Changes in metabolic profiling of sugarcane leaves induced by endophytic diazotrophic bacteria and humic acids. *PeerJ* 2018, 1–28 (2018).
50. Iriti, M. & Faoro, F. Chemical diversity and defence metabolism: How plants cope with pathogens and ozone pollution. *Int. J. Mol. Sci.* **10**, 3371–3399 (2009).
51. Barros, J. & Dixon, R. A. Plant Phenylalanine/Tyrosine Ammonia-lyases. *Trends Plant Sci.* **25**, 66–79 (2020).
52. Serra, O., Figueras, M., Franke, R., Prat, S. & Molinas, M. Unraveling ferulate role in suberin and periderm biology by reverse genetics. *Plant Signal. Behav.* **5**, 953–958 (2010).
53. Shitan, N. Secondary metabolites in plants: Transport and self-tolerance mechanisms. *Biosci. Biotechnol. Biochem.* **80**, 1283–1293 (2016).

54. Ralph, J. *et al.* Identification of the structure and origin of a thioacidolysis marker compound for ferulic acid incorporation into angiosperm lignins (and an indicator for cinnamoyl CoA reductase deficiency). *Plant J.* **53**, 368–379 (2008).
55. Faulds, C. B. & Williamson, G. The role of hydroxycinnamates in the plant cell wall. *J. Sci. Food Agric.* **79**, 393–395 (1999).
56. Wende, G., Waldron, K. W., Smith, A. C. & Brett, C. T. Tissue-specific developmental changes in cell-wall ferulate and dehydrodiferulates in sugar beet. *Phytochemistry* **55**, 103–110 (2000).
57. Sánchez, M., Peña, M. J., Revilla, G. & Zarra, I. Changes in Dehydrodiferulic Acids and Peroxidase Activity against Ferulic Acid Associated with Cell Walls during Growth of Pinus pinaster Hypocotyl. *Plant Physiol.* **111**, 941–946 (1996).
58. Jung, H. J. G. Maize stem tissues: Ferulate deposition in developing internode cell walls. *Phytochemistry* **63**, 543–549 (2003).
59. Bunzel, M., Ralph, J., Lu, F., Hatfield, R. D. & Steinhart, H. Alcohol cross-coupling products in cereal grains. *J. Agric. Food Chem.* **52**, 6496–6502 (2004).
60. Harris, P. J. & Trethewey, J. A. K. The distribution of ester-linked ferulic acid in the cell walls of angiosperms. *Phytochem. Rev.* **9**, 19–33 (2010).
61. MacAdam, J. W., Sharp, R. E. & Nelson, C. J. Peroxidase Activity in the Leaf Elongation Zone of Tall Fescue. *Plant Physiol.* **99**, 879–885 (1992).
62. Vogel, J. Unique aspects of the grass cell wall. *Curr. Opin. Plant Biol.* **11**, 301–307 (2008).
63. Riboulet, C. *et al.* Kinetics of phenylpropanoid gene expression in maize growing internodes: Relationships with cell wall deposition. *Crop Sci.* **49**, 211–223 (2009).
64. Bonawitz, N. D. & Chapple, C. The genetics of lignin biosynthesis: Connecting genotype to phenotype. *Annu. Rev. Genet.* **44**, 337–363 (2010).
65. Cesarino, I., Araújo, P., Domingues, A. P. & Mazzafera, P. An overview of lignin metabolism and its effect on biomass recalcitrance. *Rev. Bras. Bot.* **35**, 303–311 (2012).
66. Yadav, V. *et al.* Phenylpropanoid pathway engineering: An emerging approach towards plant defense. *Pathogens* **9**, 1–25 (2020).
67. De Tullio, M. C. & Arrigoni, O. Hopes, disillusions and more hopes from vitamin C. *Cell. Mol. Life Sci.* **61**, 209–219 (2004).
68. Smith, A. G., Croft, M. T., Moulin, M. & Webb, M. E. Plants need their vitamins too. *Curr. Opin. Plant Biol.* **10**, 266–275 (2007).
69. Guschina, I. A., Everard, J. D., Kinney, A. J., Quant, P. A. & Harwood, J. L. Studies on the regulation of lipid biosynthesis in plants: Application of control analysis to soybean. *Biochim. Biophys. Acta - Biomembr.* **1838**, 1488–1500 (2014).
70. Salama, K. H. A. & Mansour, M. M. F. Choline priming-induced plasma membrane lipid alterations contributed to improved wheat salt tolerance. *Acta Physiol. Plant.* **37**, 1–7 (2015).

71. Su, J. *et al.* Evaluation of the stress-inducible production of choline oxidase in transgenic rice as a strategy for producing the stress-protectant glycine betaine. *J. Exp. Bot.* **57**, 1129–1135 (2006).
72. Fagone, P. & Jackowski, S. Phosphatidylcholine and the CDP-choline cycle. *Biochim. Biophys. Acta - Mol. Cell Biol. Lipids* **1831**, 523–532 (2013).
73. Zhao, H., Tan, J. & Qi, C. Photosynthesis of Rehmannia glutinosa subjected to drought stress is enhanced by choline chloride through alleviating lipid peroxidation and increasing proline accumulation. *Plant Growth Regul.* **51**, 255–262 (2007).
74. You, L. *et al.* Accumulation of glycine betaine in transplastomic potato plants expressing choline oxidase confers improved drought tolerance. *Planta* **249**, 1963–1975 (2019).
75. Mangure, J. D. Speed of germination: aid in selection and evaluation for seedling emergence and vigor. *Crop Sci.* **2**, 176–177 (1962).
76. Giavalisco, P. *et al.* Elemental formula annotation of polar and lipophilic metabolites using 13C, 15N and 34S isotope labelling, in combination with high-resolution mass spectrometry. *Plant J.* **68**, 364–376 (2011).
77. Roessner, U. *et al.* Metabolic profiling allows comprehensive phenotyping of genetically or environmentally modified plant systems. *Plant Cell* **13**, 11–29 (2001).
78. Weckwerth, W., Wenzel, K. & Fiehn, O. Process for the integrated extraction, identification and quantification of metabolites, proteins and RNA to reveal their co-regulation in biochemical networks. *Proteomics* **4**, 78–83 (2004).
79. Cuadros-Inostroza, Á. *et al.* TargetSearch - a Bioconductor package for the efficient preprocessing of GC-MS metabolite profiling data. *BMC Bioinformatics* **10**, 1–12 (2009).
80. De Vos, R. C. H. *et al.* Untargeted large-scale plant metabolomics using liquid chromatography coupled to mass spectrometry. *Nat. Protoc.* **2**, 778–791 (2007).
81. Pluskal, T., Castillo, S., Villar-Briones, A. & Orešič, M. MZmine 2: Modular framework for processing, visualizing, and analyzing mass spectrometry-based molecular profile data. *BMC Bioinformatics* **11**, (2010).
82. Wang, M. *et al.* Sharing and community curation of mass spectrometry data with GNPS. *Nat. Biotechnol.* **34**, 828–837 (2017).
83. Xia, J., Sinelnikov, I. V., Han, B. & Wishart, D. S. MetaboAnalyst 3.0-making metabolomics more meaningful. *Nucleic Acids Res.* **43**, W251–W257 (2015).

Figures

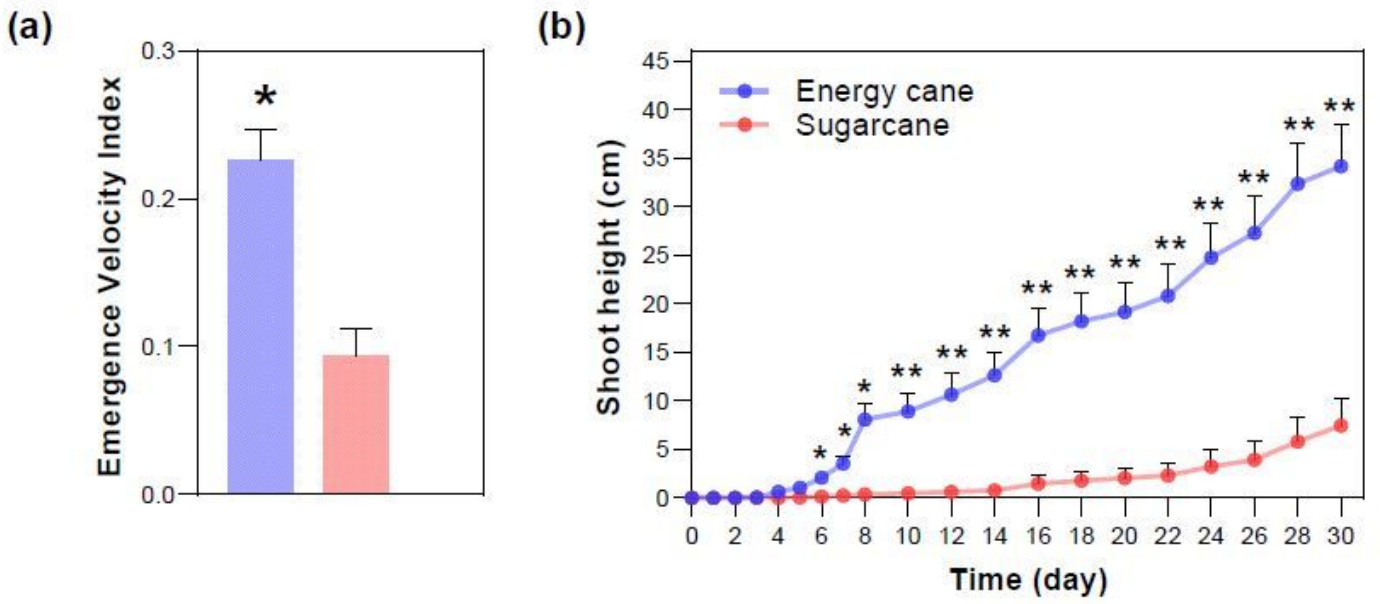

Figure 1

Evaluation sprouting rate and shoot development: Energy cane and Sugarcane. (a) Emergence velocity index (EVI). (b) Shoot height. Blue and red colors represent energy cane and sugarcane, respectively. Data are expressed as the mean and standard error of the mean (SEM). The statistically significant difference between cultivars, analyzed by the T-test (P <0.05%).

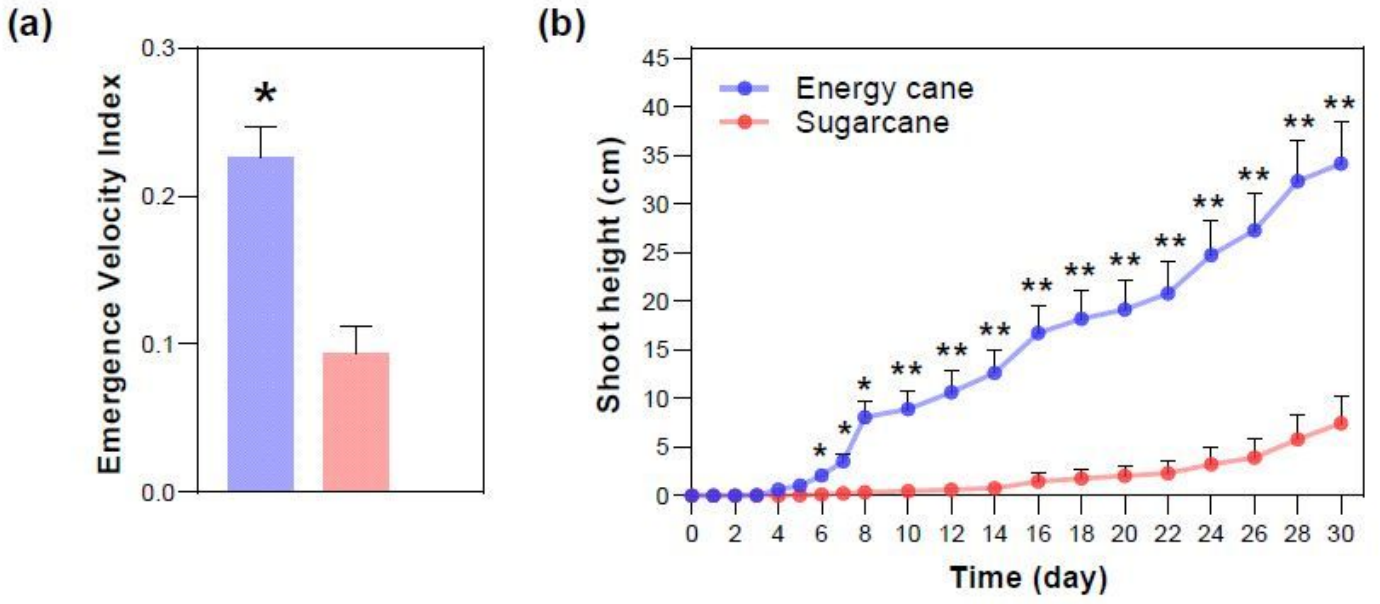

Figure 1

Evaluation sprouting rate and shoot development: Energy cane and Sugarcane. (a) Emergence velocity index (EVI). (b) Shoot height. Blue and red colors represent energy cane and sugarcane, respectively. Data are expressed as the mean and standard error of the mean (SEM). The statistically significant difference between cultivars, analyzed by the T-test (P <0.05%).

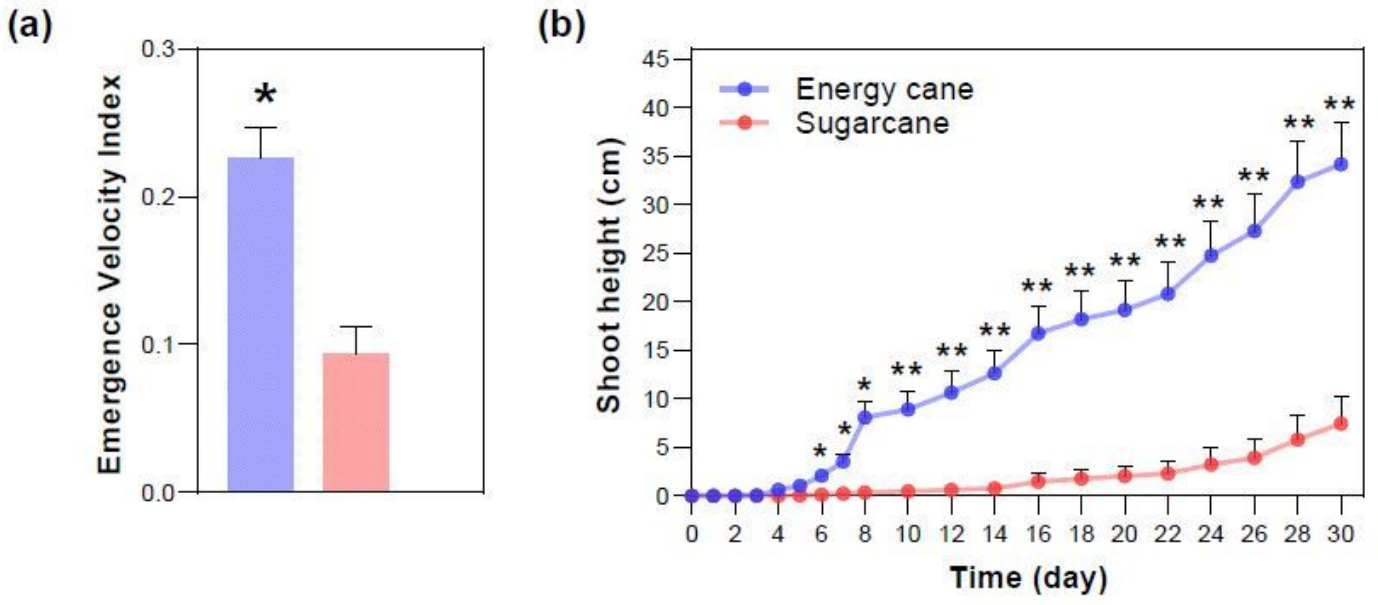

Figure 2

Evaluation sprouting rate and shoot development: Energy cane and Sugarcane. (a) Emergence velocity index (EVI). (b) Shoot height. Blue and red colors represent energy cane and sugarcane, respectively. Data are expressed as the mean and standard error of the mean (SEM). The statistically significant difference between cultivars, analyzed by the T-test (P <0.05%).

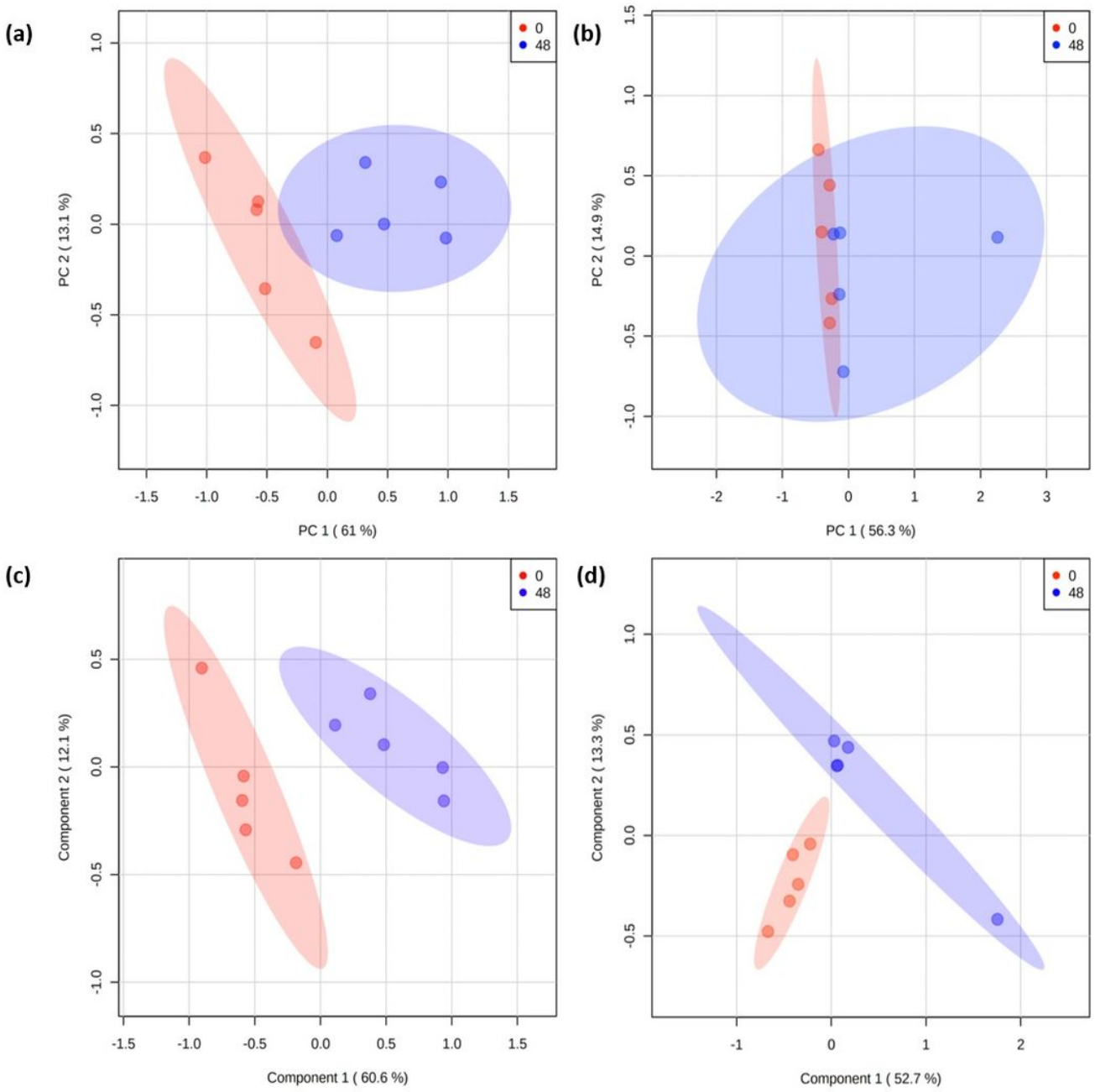

Figure 2

Principal component analysis (PCA) of metabolite profiles by GC-TOF-MS during the axillary bud outgrowth of (a) energy cane and (b) sugarcane, at 0 and 48 hours. PCA presented as a combination of the two dimensions, which together represent 74.1% and 71.2% of the variance of the metabolites of energy cane and sugarcane, respectively. Partial least square-discrimination analysis (PLS-DA) of metabolite profiles by GC-TOF-MS during the axillary bud outgrowth of (c) energy cane and (d) sugarcane, in the times of 0 and 48 hours. PLS-DA presented as a combination of the two dimensions, which together represent 72.7% and 66% of the variance of the metabolites of energy cane and sugarcane, respectively.

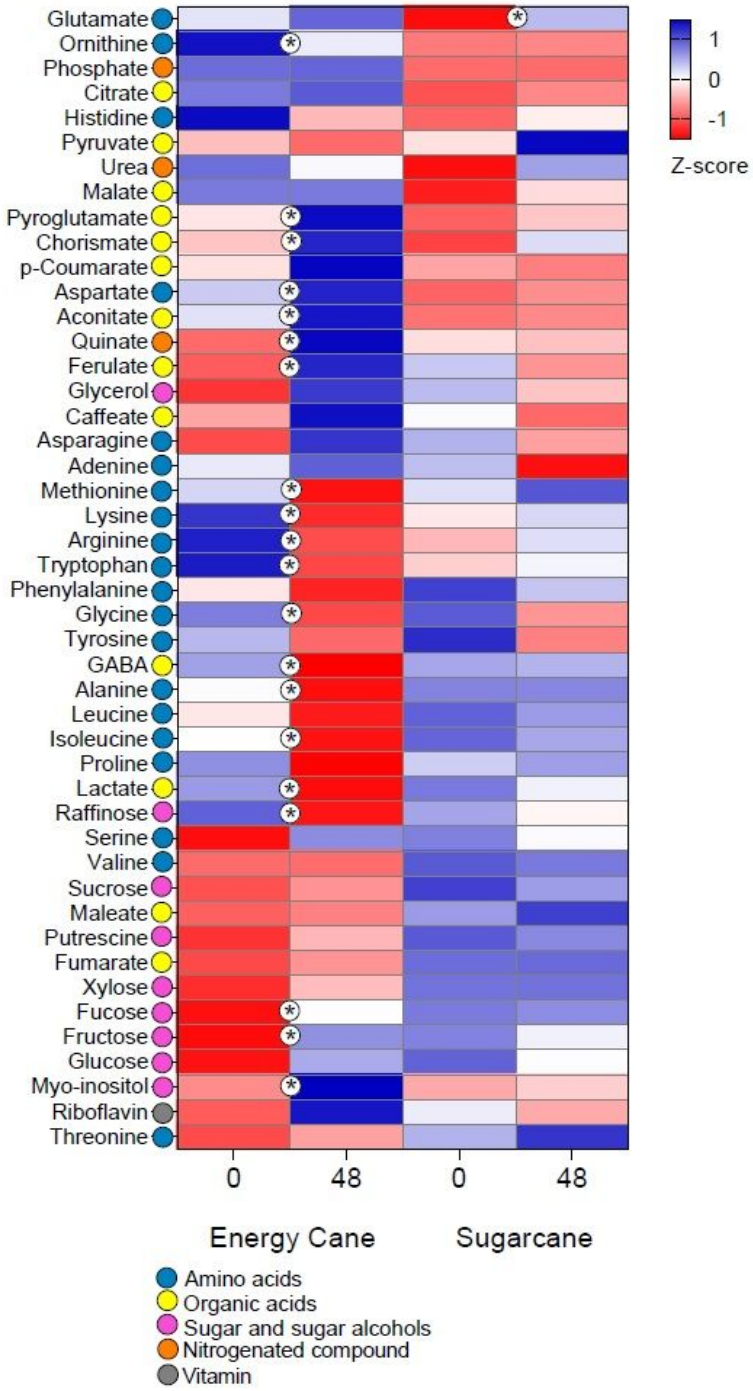

Figure 3

Metabolites identified by GC-TOF-MS during the axillary bud outgrowth of energy cane and sugarcane. Heatmap was built using log2 followed by the normalization of metabolites by z-score. Blue scale indicates major and minor red, relative concentration. A total of five biological replicas were used, each replica was composed of a pool of five buds. Circle with an asterisk represents a significant difference between the times of 0 and 48 hours for each cultivar, using the Student T-test ($p \leq 0.05$).

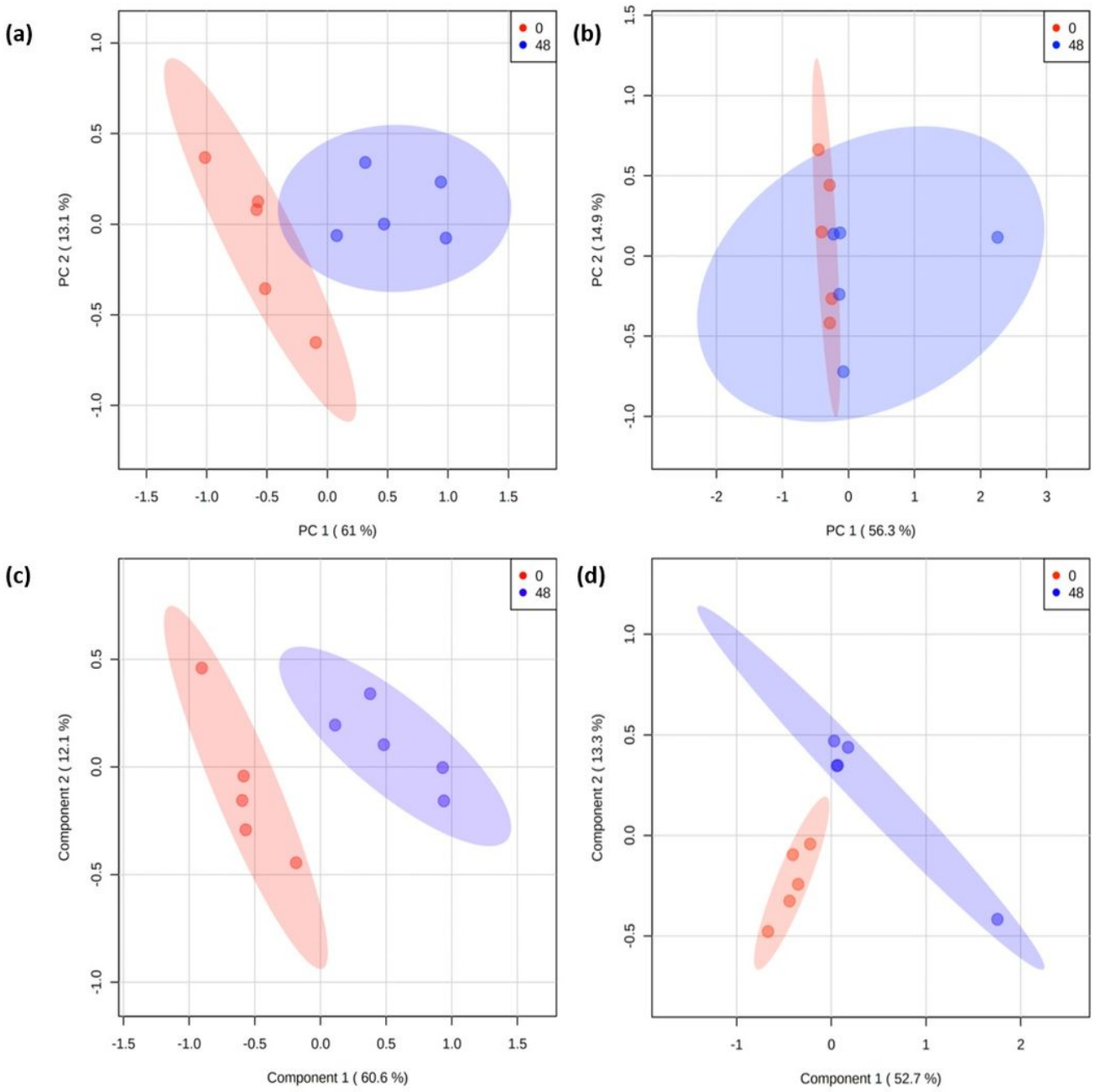

Figure 3

Principal component analysis (PCA) of metabolite profiles by GC-TOF-MS during the axillary bud outgrowth of (a) energy cane and (b) sugarcane, at 0 and 48 hours. PCA presented as a combination of the two dimensions, which together represent 74.1% and 71.2% of the variance of the metabolites of energy cane and sugarcane, respectively. Partial least square-discrimination analysis (PLS-DA) of metabolite profiles by GC-TOF-MS during the axillary bud outgrowth of (c) energy cane and (d) sugarcane, in the times of 0 and 48 hours. PLS-DA presented as a combination of the two dimensions, which together represent 72.7% and 66% of the variance of the metabolites of energy cane and sugarcane, respectively.

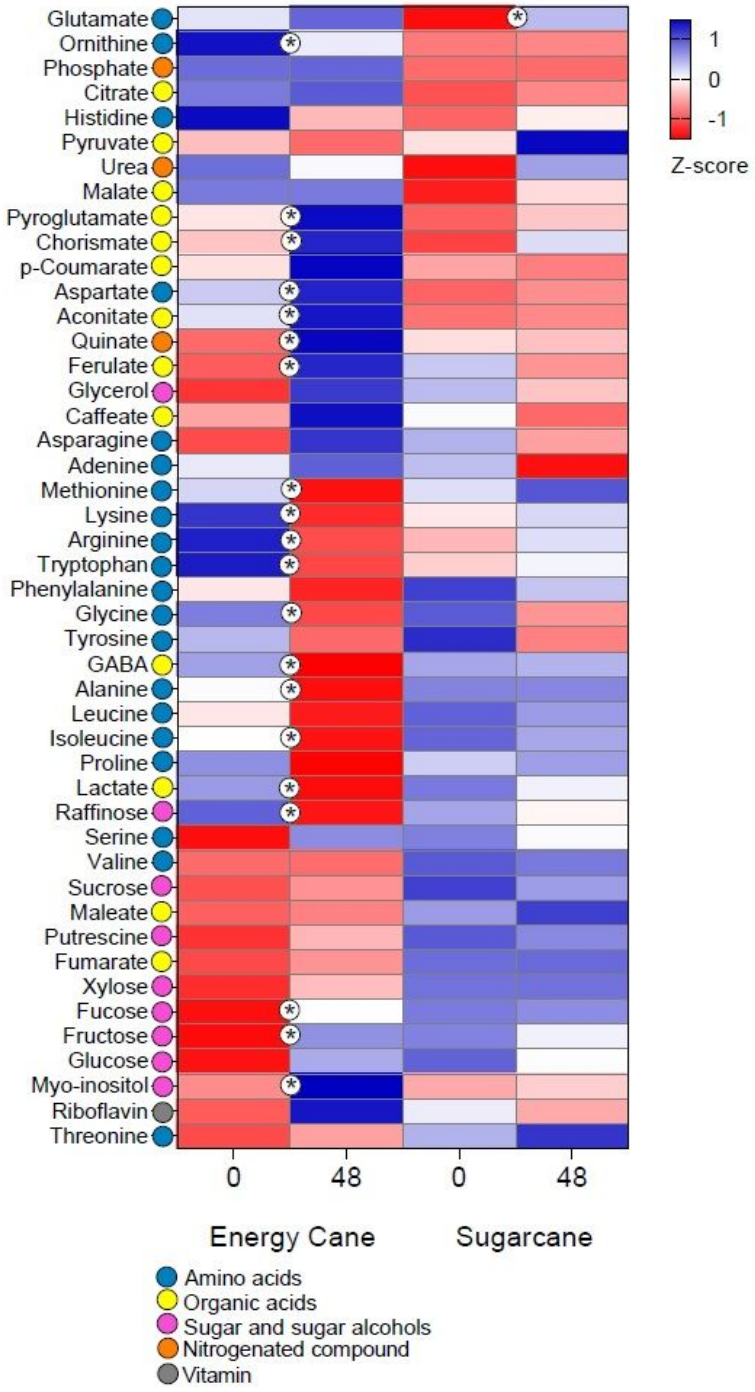

Figure 3

Metabolites identified by GC-TOF-MS during the axillary bud outgrowth of energy cane and sugarcane. Heatmap was built using log2 followed by the normalization of metabolites by z-score. Blue scale indicates major and minor red, relative concentration. A total of five biological replicas were used, each replica was composed of a pool of five buds. Circle with an asterisk represents a significant difference between the times of 0 and 48 hours for each cultivar, using the Student T-test ($p \leq 0.05$).

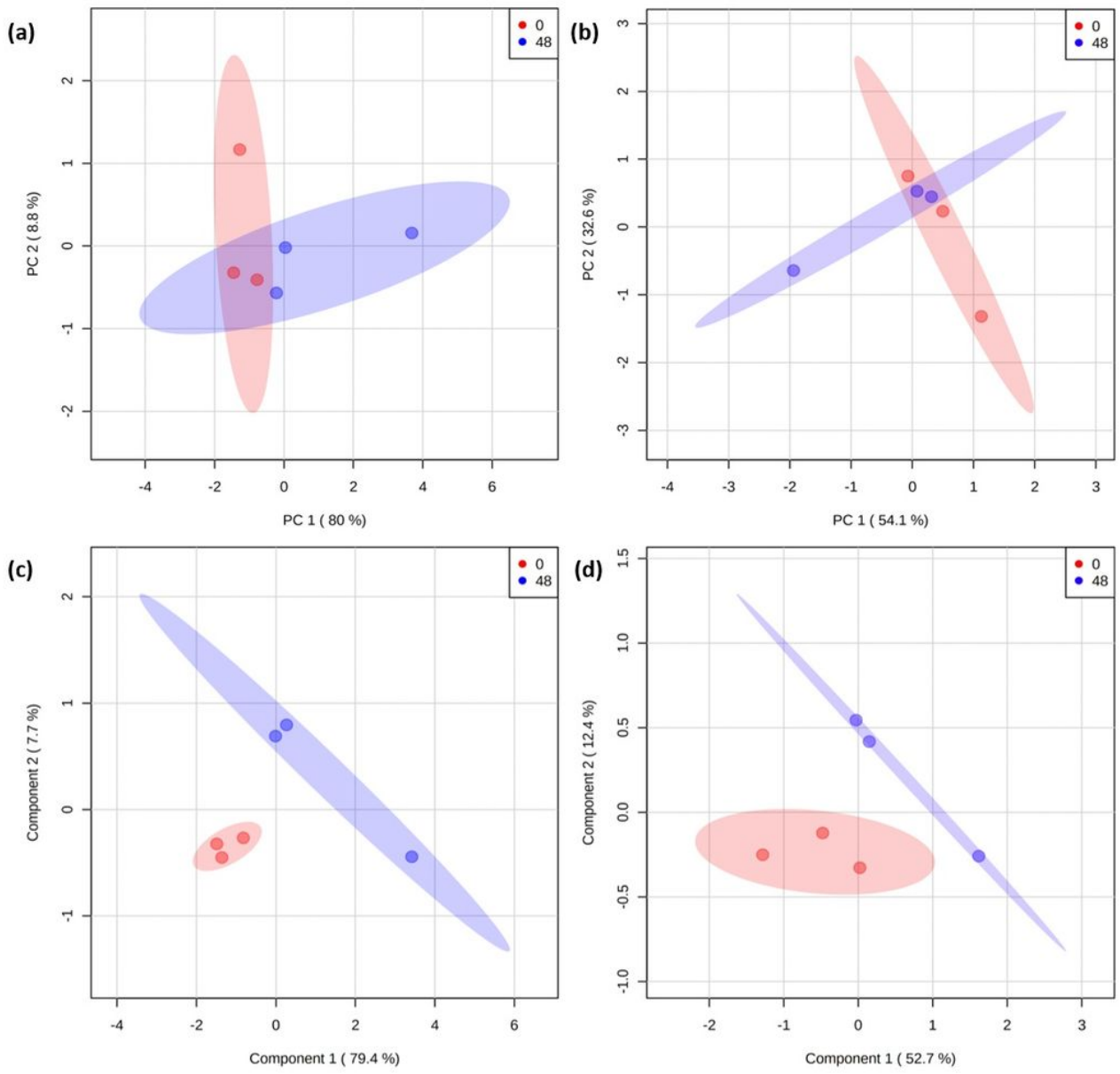

Figure 5

Principal component analysis (PCA) of metabolite profiles by LC-ESI(+)-MS/MS during the axillary bud outgrowth of (a) energy cane and (b) sugarcane, at 0 and 48 hours. PCA presented as a combination of the two dimensions, which together represent 88.8% and 86.7% of the variance of the metabolites of energy cane and sugarcane, respectively. Partial least square-discrimination analysis (PLS-DA) of metabolite profiles by LC-ESI(+)-MS/MS during the axillary bud outgrowth of (c) energy cane and (d) sugarcane, in the times of 0 and 48 hours. PLS-DA presented as a combination of the two dimensions, which together represent 87.1% and 65.1% of the variance of the metabolites of energy cane and sugarcane, respectively.

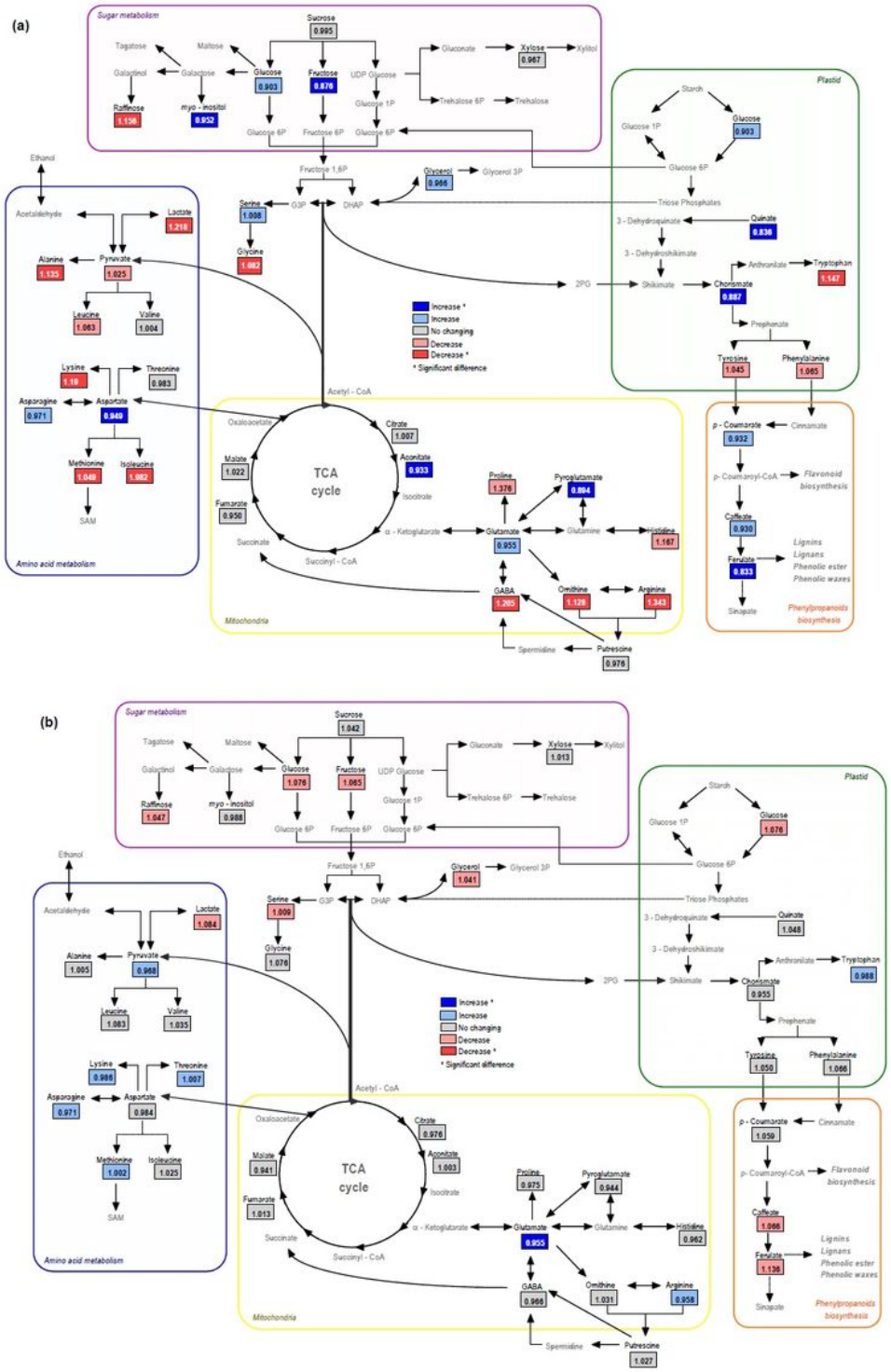

Figure 5

Metabolic map during the axillary bud outgrowth, which describes the fold change ($p \leq 0.05$) in metabolites at 0 and 48 hours for (a) energy cane and (b) sugarcane. The undetected metabolites are indicated by gray, the metabolites detected by black. Blue boxes indicate higher and lower red abundant levels of metabolites, in gray that there were no changes. Asterisk shows significant difference in the concentration of metabolites during bud outgrowth.

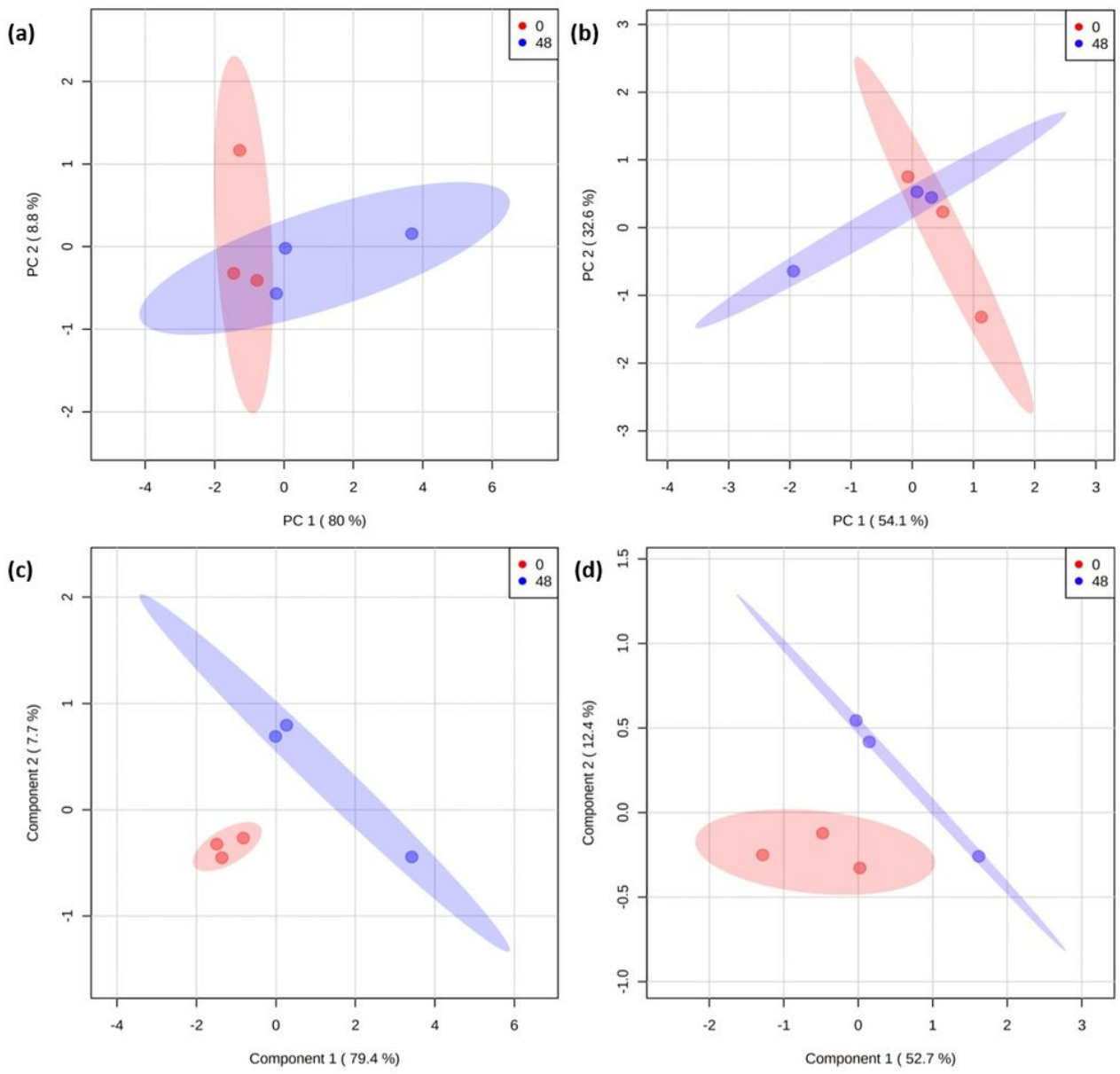

Figure 5

Principal component analysis (PCA) of metabolite profiles by LC-ESI(+)-MS/MS during the axillary bud outgrowth of (a) energy cane and (b) sugarcane, at 0 and 48 hours. PCA presented as a combination of the two dimensions, which together represent 88.8% and 86.7% of the variance of the metabolites of energy cane and sugarcane, respectively. Partial least square-discrimination analysis (PLS-DA) of metabolite profiles by LC-ESI(+)-MS/MS during the axillary bud outgrowth of (c) energy cane and (d) sugarcane, in the times of 0 and 48 hours. PLS-DA presented as a combination of the two dimensions, which together represent 87.1% and 65.1% of the variance of the metabolites of energy cane and sugarcane, respectively.

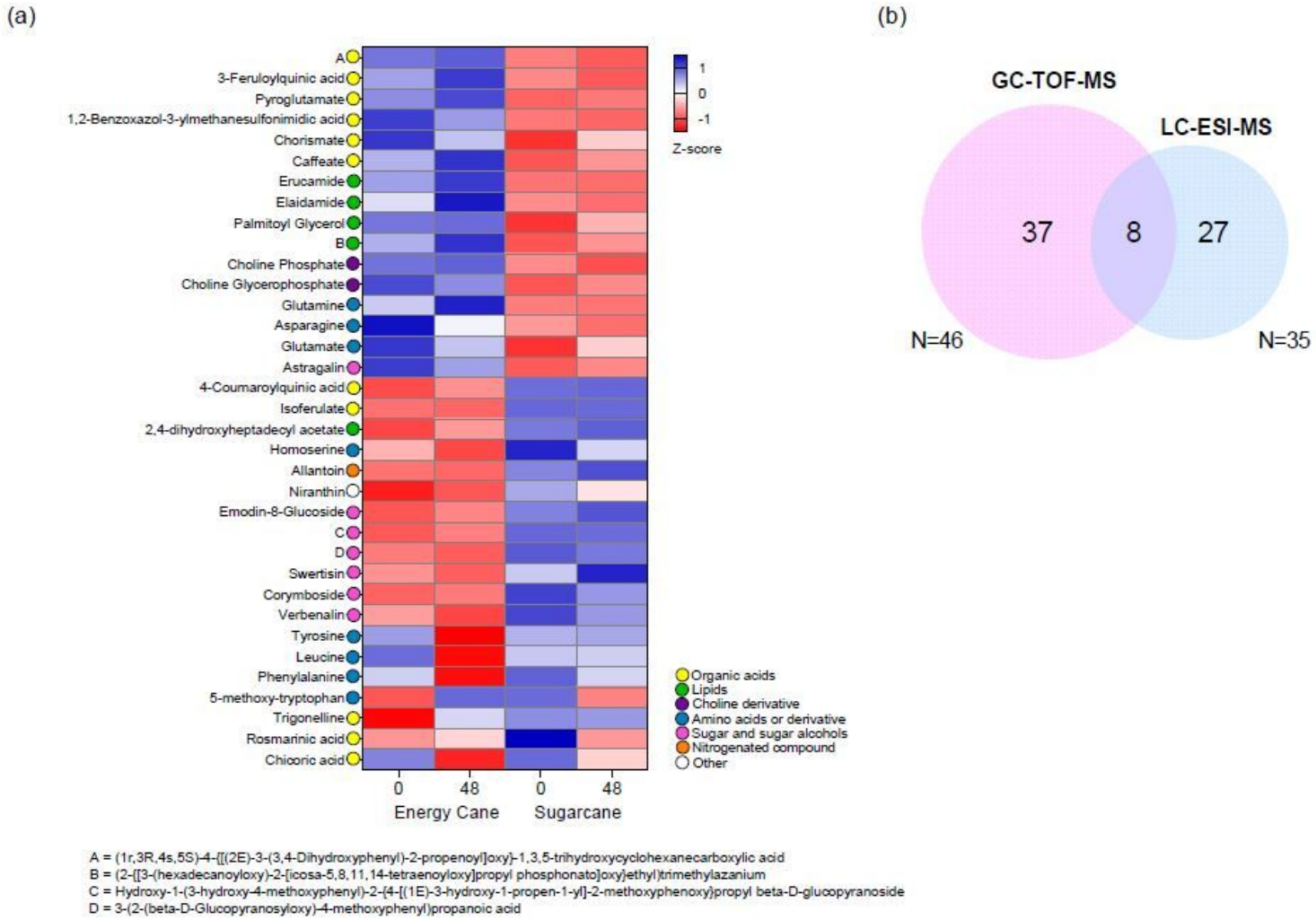

Figure 6

Metabolites identified by LC-ESI(+)-MS/MS during the axillary bud outgrowth of energy cane and sugarcane. Heatmap was built using log2 followed by the normalization of metabolites by z-score. Blue scale indicates major and minor red, relative concentration. A total of three biological replicas were used, each replica was composed of a pool of five gems. Two-way ANOVA analysis demonstrate significant difference between cultivar and time interactions (p-value = 0.00181).

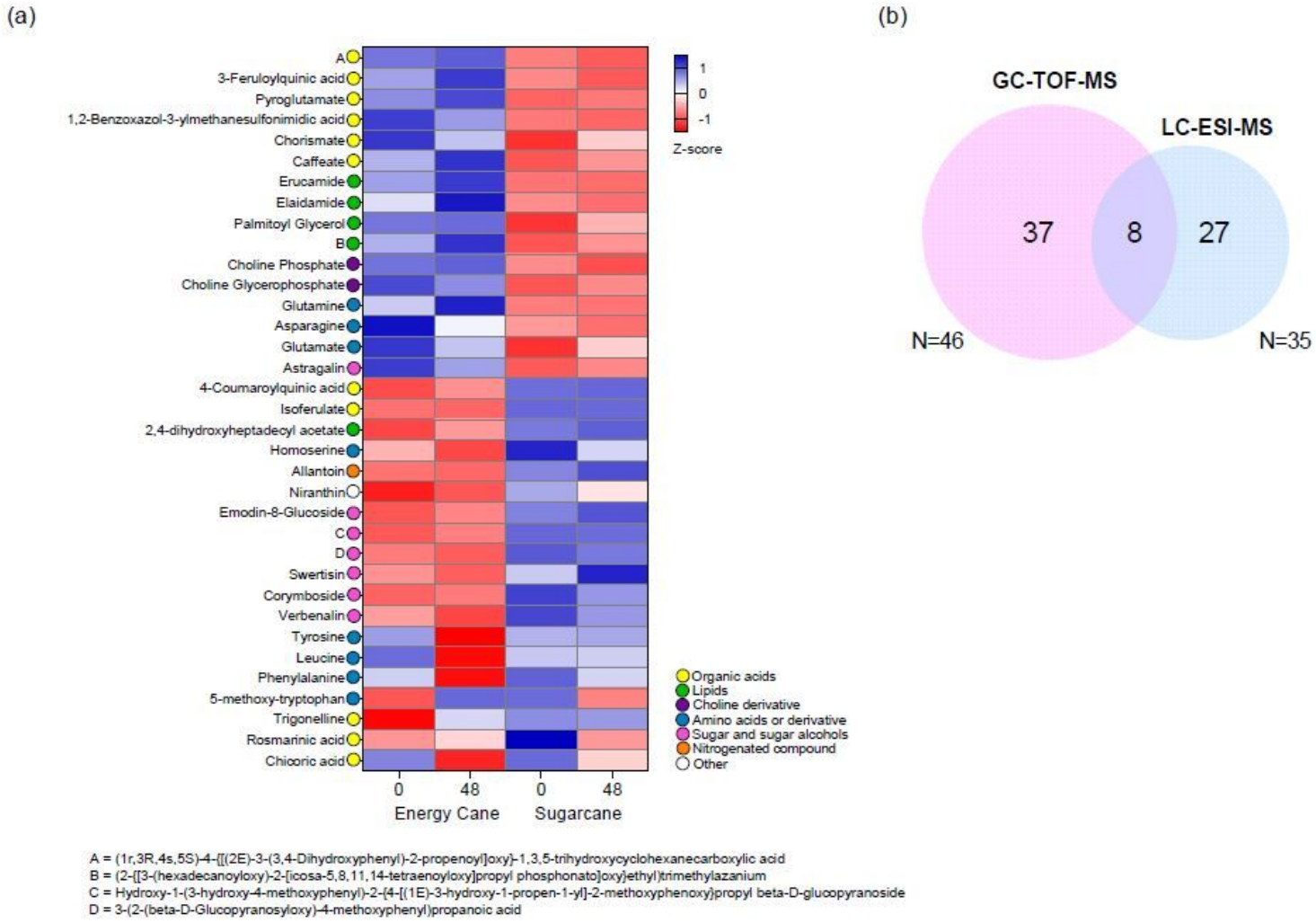

Figure 6

Metabolites identified by LC-ESI(+)-MS/MS during the axillary bud outgrowth of energy cane and sugarcane. Heatmap was built using log2 followed by the normalization of metabolites by z-score. Blue scale indicates major and minor red, relative concentration. A total of three biological replicas were used, each replica was composed of a pool of five gems. Two-way ANOVA analysis demonstrate significant difference between cultivar and time interactions (p-value = 0.00181).

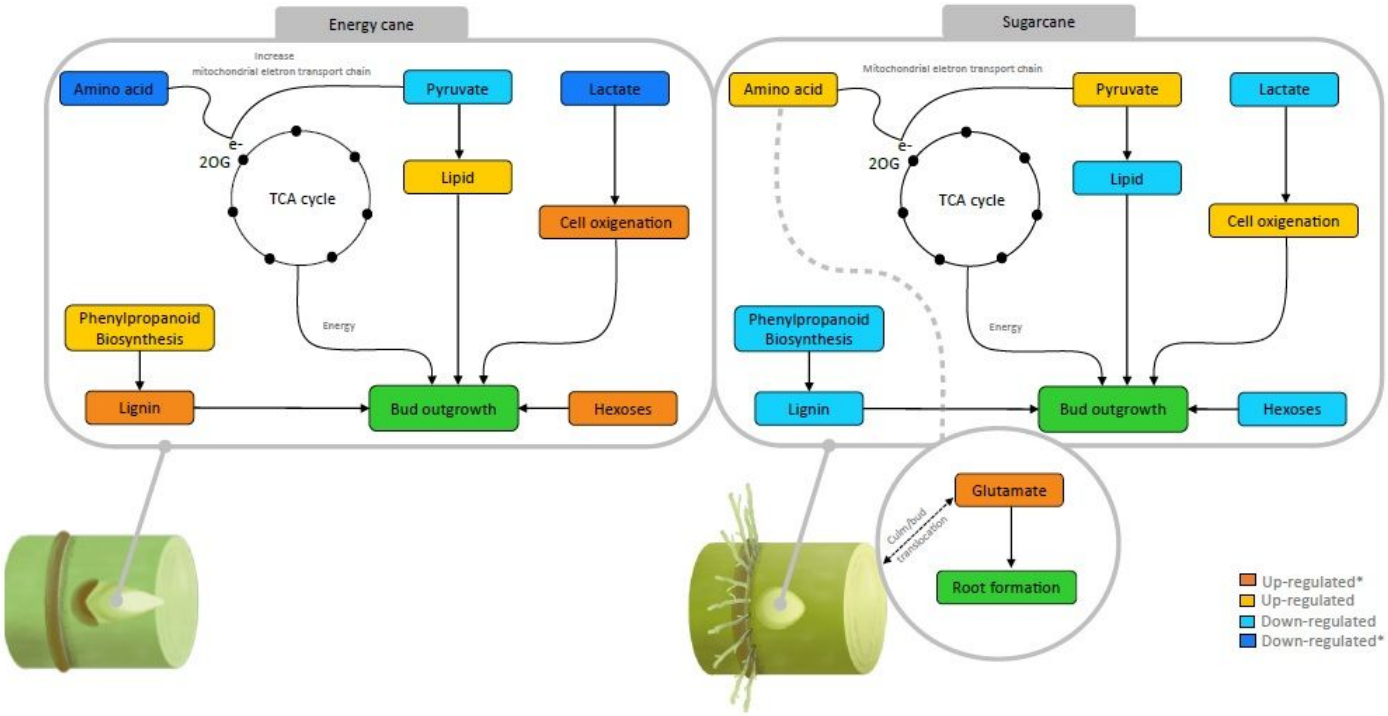

Figure 7

Schematic representation of the main changes during the axillary bud outgrowth of energy cane and sugarcane In cane energy, an increase in hexoses, a reduction in pyruvate levels and the catabolism of some amino acids was observed, resulting in an increase in the electron transport chain in the TCA cycle. There was an increase in the levels of lipids and compounds related to the phenylpropanoid pathway, which led to an increase in membrane and cell wall formation. In sugarcane, a reduction in the levels of hexoses, an increase in the levels of pyruvate and amino acids was observed. There was an increase in glutamate, which acts as a signaling molecule between the bud and culm tissues, and leads to the formation of root in the setts. In both cultivars there was a reduction in lactate levels (most evident in energy cane), which leads to an increase in cellular oxygenation, which may be an indication for rapid shoot development in energy cane, while in sugarcane occurs root formation in the setts, which may be related to high levels of glutamate.

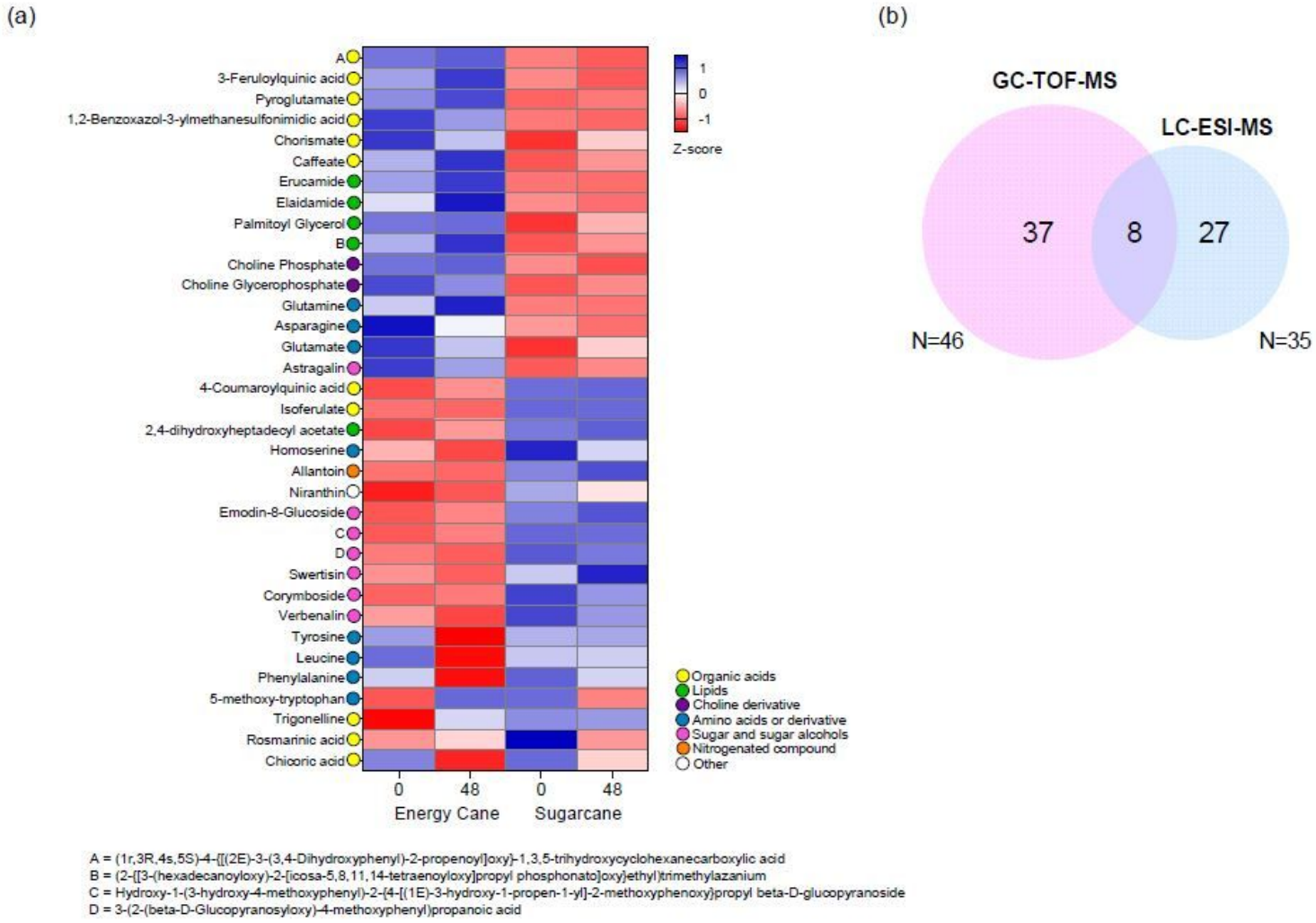

Figure 7

Metabolites identified by LC-ESI(+)-MS/MS during the axillary bud outgrowth of energy cane and sugarcane. Heatmap was built using log2 followed by the normalization of metabolites by z-score. Blue scale indicates major and minor red, relative concentration. A total of three biological replicas were used, each replica was composed of a pool of five gems. Two-way ANOVA analysis demonstrate significant difference between cultivar and time interactions (p-value = 0.00181).

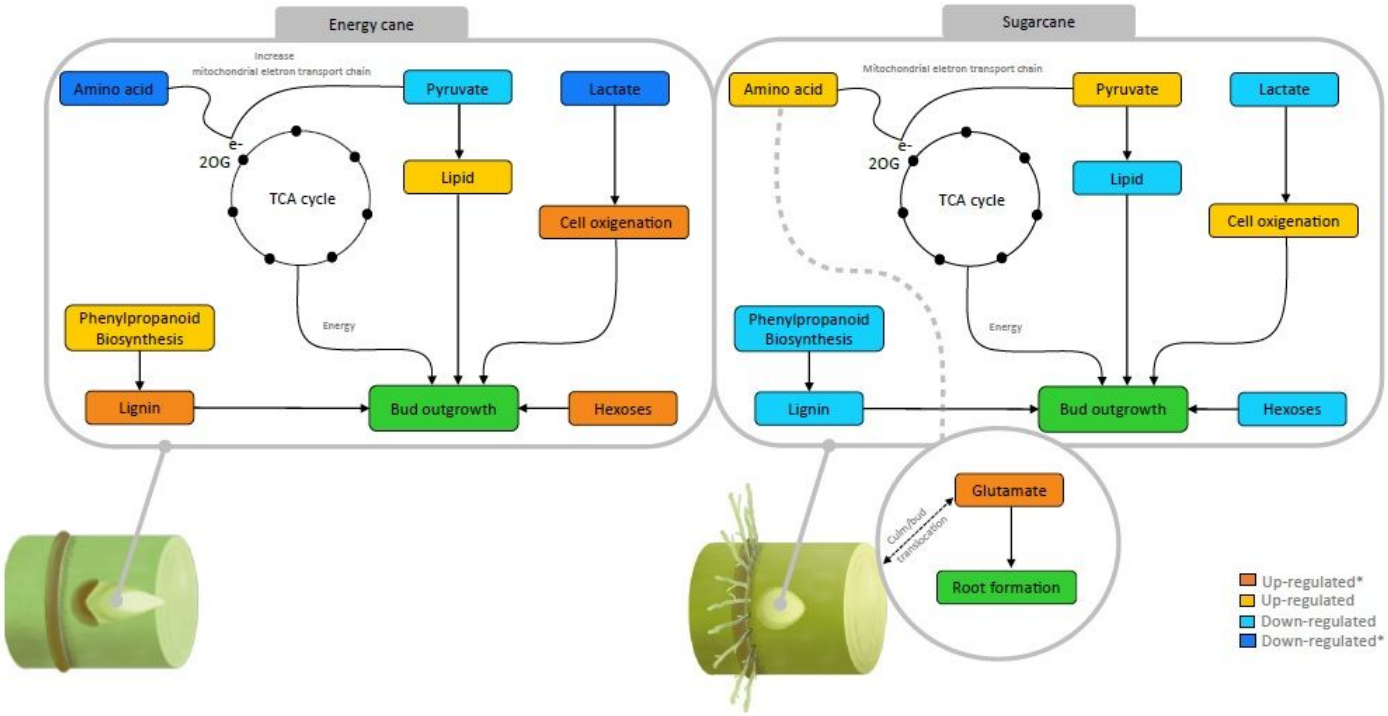

Figure 8

Schematic representation of the main changes during the axillary bud outgrowth of energy cane and sugarcane In cane energy, an increase in hexoses, a reduction in pyruvate levels and the catabolism of some amino acids was observed, resulting in an increase in the electron transport chain in the TCA cycle. There was an increase in the levels of lipids and compounds related to the phenylpropanoid pathway, which led to an increase in membrane and cell wall formation. In sugarcane, a reduction in the levels of hexoses, an increase in the levels of pyruvate and amino acids was observed. There was an increase in glutamate, which acts as a signaling molecule between the bud and culm tissues, and leads to the formation of root in the setts. In both cultivars there was a reduction in lactate levels (most evident in energy cane), which leads to an increase in cellular oxygenation, which may be an indication for rapid shoot development in energy cane, while in sugarcane occurs root formation in the setts, which may be related to high levels of glutamate.

Supplementary Files

This is a list of supplementary files associated with this preprint. Click to download.

- Supplementaryinformation.pdf
- Supplementaryinformation.pdf

- TableS1.xlsx
- TableS1.xlsx
- TableS2.xlsx